PROCEEDINGS of the
23rd International Congress on Acoustics

9 to 13 September 2019 in Aachen, Germany

Estimation of infrasound source positions using multipoint observation

Zhenglie CUI[1], Ryosuke SASAHARA[1], Ryouichi NISHIMURA[2], Yôiti SUZUKI[1]

[1] Research Institute of Electrical Communication, Tohoku University, Japan

[2] Resilient ICT Research Center, National Institute of Information and Communications Technology, Japan

ABSTRACT

Infrasound can be excited by global phenomena such as *tsunamis* and volcanic eruptions. Because infrasound travels significantly faster in the atmosphere than *tsunami* gravity waves, early detection of tsunamis can be achieved by monitoring the infrasound. To accurately identify a *tsunami* source (i.e., the position of the infrasound source), using numerous sensors distributed with long baselines is important. We developed a low-cost infrasound observation device using micro-electro-mechanical systems-based atmospheric pressure sensors. To test its usability, indoor and outdoor tests were conducted using multipoint observations. In the indoor experiments, the infrasound was excited by opening and closing a door and by bursting a large balloon. The accuracy of time synchronization was examined by setting the infrasound observation devices across different points in a room. The results demonstrated that the errors in time synchronization are tolerable. In the outdoor field test, the infrasound excited by fireworks during a festival was observed at multiple points in Sendai, Japan. Furthermore, as a large-scale infrasound observation experiment, we measured the infrasound excited by volcanic eruptions in Sakurajima, Japan. The results showed that the source position can be estimated with reasonable accuracy for an infrasound with an amplitude of over 5 Pa (waveform noise). This suggests the potential suitability of the device in estimating the source position of *tsunami*-scale earthquakes.

Keywords: Infrasound, Atmospheric pressure sensor, Source position estimation

1. INTRODUCTION

Large-scale disasters such as strong earthquakes, huge oceanic gravity waves (*tsunamis*), and volcanic eruptions often generate sound waves, the frequency spectra of which have components below the human audible frequency range (i.e., below 20 Hz) [1]-[3]. Such a low-frequency sound is called infrasound, which is analogous to infrared radiation emitted in the form of low-frequency light. Infrasound travels at approximately the speed of sound, i.e., in the range of 310–343 m/s, at 20°C in the atmosphere, whereas a *tsunami* wave travels at a speed of 221 m/s at an oceanic depth of 5000 m along the ocean surface [4], and its speed reduces as it approaches the coast because the speed is proportional to the square root of the ocean depth. Consequently, the infrasound waves generated by *tsunamis* will reach the coast earlier than the *tsunami* waves. Furthermore, the infrasound generated by *tsunamis* provides information on the shape and wavelength of the *tsunami* waves [5][6].

As infrasound in atmosphere travels significantly faster than *tsunamis*, early detection of *tsunamis* can be achieved by monitoring the infrasound [7][8]. To accurately identify the source positions of *tsunamis* as those of infrasound sources, installing numerous sensors distributed along the coast with long baselines is necessary. However, constructing new infrasound monitoring networks will be expensive since traditional infrasound sensors (micro-barometers) are expensive.

Therefore, in our previous study [9], we developed a small infrasound observation device using a low-cost atmospheric pressure sensor (BME280 BOSCH) based on micro-electric mechanical systems (MEMS) technology and a microcomputer (Raspberry Pi 3, Raspberry Pi Fund). A field test was carried out to evaluate the usability of the device by deploying it 13 km away from an active volcano (Sakurajima in Japan). The results showed that the low-cost device can be used to observe

[1] sai@ais.riec.tohoku.ac.jp, yoh@riec.tohoku.ac.jp
[2] ryou@nict.go.jp

Figure 1 – New infrasound observation device comprising eight MEMS pressure sensors

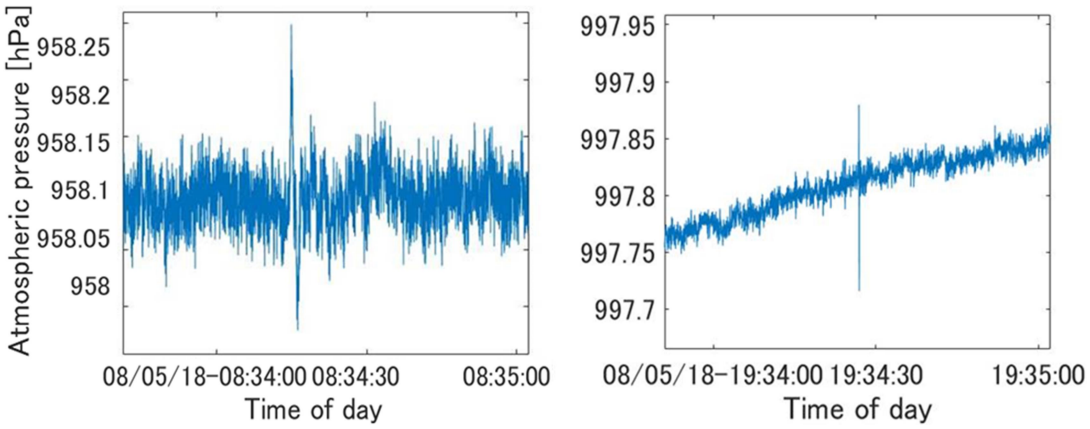

(a) (b)

Figure 2 – Noise test waveform results of (a) old device and (b) new device

infrasound waves at frequencies down to 0.01 Hz, similar to how a conventional micro-barometer is used. Moreover, it enables the detection of a signal with a peak-to-peak amplitude of around if the signal level is sufficiently high, e.g., more than 10 Pa.

However, the noise level and thus the error were much higher in the higher frequency range. Therefore, in the present study, to improve the signal-to-noise ratio (S/N), eight MEMS pressure sensors were stacked on a single board to assemble a new infrasound monitoring device. To test its performance, indoor and outdoor experiments were conducted using multipoint observations. In this article, we introduce the outline of the new device and report the experimental results.

2. NEW INFRASOUND OBSERVATION DEVICE

Figure 1 shows the external appearance of the new infrasound observation device, which consists of eight MEMS barometric pressure sensors (BME 280, BOSCH), a microcomputer (Raspberry Pi, Raspberry Pi Fund), and a GPS base. The device uses the eight MEMS sensors to improve the SN ratio by averaging the eight output signals. To make the device compact, the modules were designed to fit in a case of dimensions 12 cm (width) × 12 cm (depth) × 10 cm (height). For the measurement, after synchronizing the time with GPS, an infrasound is recorded as the temporal change in the atmospheric pressure at a sampling rate ranging from 1 to 50 Hz with 16-bit quantization.

Figure 2 shows the results of the noise test waveform obtained using the device at a sampling rate of 50 Hz. Compared with a previous test waveform based on only one MEMS pressure sensor [9], the waveform noise is reduced by approximately 10 dB (low-pass filter of 256 order and a cutoff frequency of 20 Hz). The results show that the new device enables the detection of a signal with a peak-to-peak amplitude in the range of approximately 5–6 Pa. This means that it is possible to sense infrasound if the peak-to-peak sound pressure level is approximately 108 dB or more.

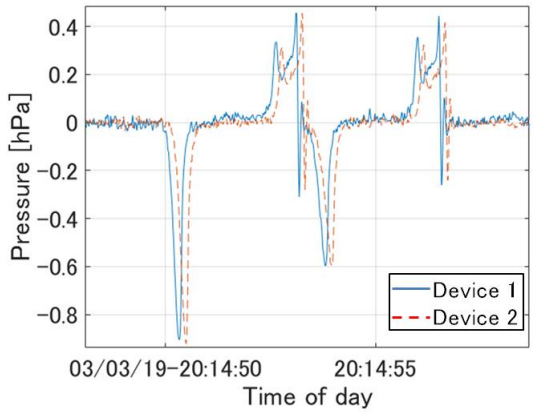

Figure 3 – Comparison of infrasound waveforms (Comparison of infrasound waveforms generated by door opening/closing between two devices)

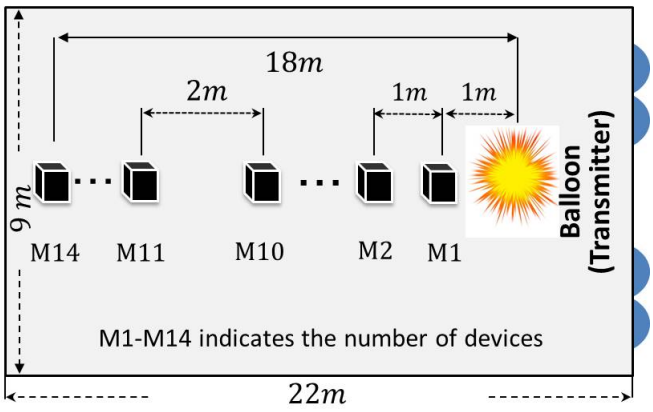

Figure 4 – Experiment environment (Comparison of time waveforms between two devices)

3. EXPERIMENT 1: INDOOR EXPERIMENTS

3.1 Verification of time synchronization

The time synchronization between the devices was tested using two devices when the infrasound was generated. The experiment was conducted in a soundproof room at the Research Institute of Electrical Communication, Tohoku University. The infrasound was excited by opening and closing a door to change the atmospheric pressure in the room. The device was set adjacent on a desk placed in the soundproof room, and the measurement was conducted by opening and closing the door twice in 10 s.

The DC component was removed by subtracting the average value of the signal. The time difference between the sensors was calculated from the phase restriction correlation after the resampling was carried out at 100 Hz (the original sampling frequency was 50 Hz). As a result, the time difference ranged from a minimum of 3 ms to a maximum of 152 ms. Figure 3 shows the infrasound waveforms when the time difference is maximum. This confirms an accuracy of less than one sample point between two devices.

3.2 Estimation of distance between devices

To accurately estimate the sound source position, the infrasound signals should be recorded with correct time differences between the devices. Therefore, we checked the arrival time differences of the infrasound when opening and closing the door using the multiple observation devices and estimated the distance differences between these devices. As shown in Figure 4, 14 devices are distributed in line at intervals of 1 or 2 m in a quiet room at the Research Institute of Electrical Communication, Tohoku University (room size is 22.0 m × 9.7 m). As the infrasound generated by opening and closing the room door did not exhibit clear peaks, in this experiment, a pulsive infrasound was generated by bursting a large balloon (90 cm in diameter at the inflated state).

The peak signal was confirmed by bursting large balloons in multiple devices. The speed of sound was calculated using the relationship $331.5 + 0.6\,t$ [m/s], where t is the temperature in degree Celsius; the temperature was 16°C in the experiment. The distance between the observation devices was estimated from the arrival time difference between two of the 14 devices. As the sampling timings of each device are different, the difference in the arriving times was calculated by performing resampling at 100 Hz, and the phase difference of each peak signal was then calculated.

Table 1 lists the experimental results. For an actual interval of 17 m between M1 and M14, the estimated distance was 14.6 m as the arrival time difference was 0.04 s, resulting in an error of 2.4 m. The results showed that the time errors are tolerable because these devices are used at a sampling rate of 50 Hz. On the contrary, the estimated distance between M1 and M11 showed a large error of 49.8 m. This might be an artifact due to the reflected waves in the room and/or asynchronization due to the lack of GPS radio waves; this is a subject for future study. Except for this case, the distances between the devices could be acquired with acceptable accuracy when the distance between the devices is 15 m or more. Therefore, the device exhibits an acceptable accuracy for sensing large-scale natural disasters such as *tsunamis* and volcanic eruptions.

Table 1 – Examples of estimation results for distance between devices

Comparison data (Device number)	Arrival time difference (s)	Estimated distance (m)	Actual interval (m)	Error (m)
M1-M14	4.3×10^{-2}	14.6	17	–2.4
M1-M13	5.3×10^{-2}	15.8	15	+0.8
M1-M11	17.8×10^{-2}	60.8	11	+49.8
M6-M13	3.9×10^{-2}	13.2	10	+3.2
M7-M12	2.0×10^{-2}	6.8	7	–0.2

4. EXPERIMENT 2: OUTDOOR FIELD TEST

4.1 Observation of infrasound due to explosion of fireworks

Using the 18 new devices, we measured the infrasound excited by the explosion of fireworks during a festival at multiple points in Sendai, Japan, from 19:00 to 20:30 on August 5, 2018. As shown in Figure 5, two devices are set at each of the nine observation points from A to I around the fireworks venue. In the figure, the observation point is indicated by two-dimensional coordinates, the origin of which is the fireworks launch site. Table 2 lists the distance coordinate values of the nine points.

Figure 6 shows the observation results of the two devices C1 and C2 set at the measurement point C, as an example of the experimental results. The most significant peaks are observed at around 19:24:30 at point C, as shown in Fig. 6. Similar peak signals are also observed at both points D and E. Moreover, this peak signal, which was judged as an infrasound generated by an explosion of a firework, could not be observed at points other than C, D, and E.

The source position was thus estimated using the arrival time difference between each device, using only six data points from the observation points C, D, and E, where the peak could be observed. Specifically, with Equation (1), which was used in a previous study [10], the sound source position (u, v, d) was estimated using the sound source position (u, v), distance d (distance from the sound source to the shortest observation point), and sound speed c. In Equation (1), T_{ij} (i, j = 1-6) indicates the peak time difference between devices i and j, and (X_i, Y_j) indicates each observation point. As a result, the coordinate (u, v) was found to be (–288, –92), located 290 m away from the actual fireworks launch position. This error may be attributable to the two-dimensional estimation while a three-dimensional sound source estimation would be necessary to obtain better estimates for the explosion points in the air a few hundred meters above the ground.

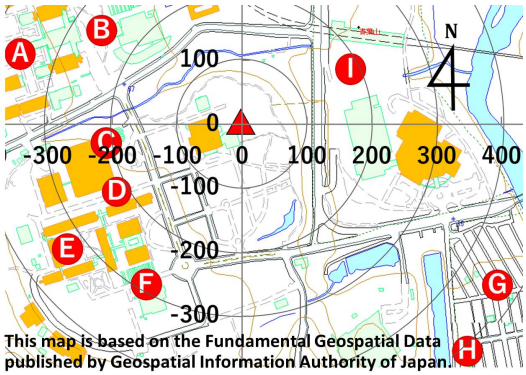

Figure 5 – Position of nine observation points A–I (the triangles represent the launch position, and the numerical values represent the distance from the launch point [m]

Table 2 – Position of observation points

Measurement point	Coordinates (m)	Distance from sound source (m)	Measurement point	Coordinates (m)	Distance from launch point (m)
A	(–336, 99)	350	F	(–138, –250)	286
B	(–214, 144)	258	G	(403, –254)	476
C	(–208, –48)	207	H	(345, –370)	506
D	(–191, –114)	222	I	(176, 87)	196
E	(–276, –191)	336			

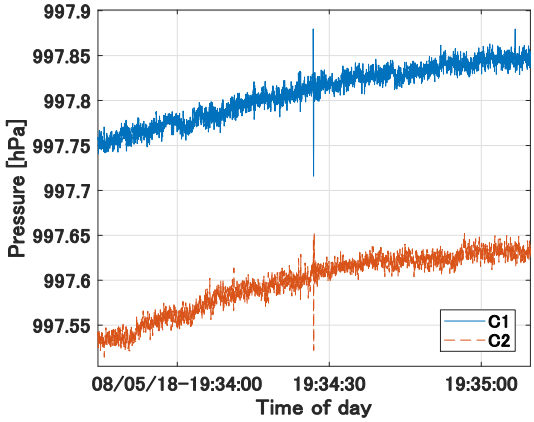

Figure 6 – Observation results for the two devices C1 and C2

$$\begin{pmatrix} 2(x_1-x_2) & 2(y_1-y_2) & -2\Delta T_{12} \\ 2(x_1-x_3) & 2(y_1-y_3) & -2\Delta T_{13} \\ 2(x_1-x_4) & 2(y_1-y_4) & -\Delta T_{14} \\ 2(x_1-x_5) & 2(y_1-y_5) & -2\Delta T_{15} \\ 2(x_1-x_6) & 2(y_1-y_6) & -2\Delta T_{16} \end{pmatrix} * \begin{pmatrix} u \\ v \\ d \end{pmatrix} = \begin{pmatrix} c^2\Delta T_{12}^2 + x_1^2 + y_1^2 - x_2^2 - y_2^2 \\ c^2\Delta T_{13}^2 + x_1^2 + y_1^2 - x_3^2 - y_3^2 \\ c^2\Delta T_{14}^2 + x_1^2 + y_1^2 - x_4^2 - y_4^2 \\ c^2\Delta T_{15}^2 + x_1^2 + y_1^2 - x_5^2 - y_5^2 \\ c^2\Delta T_{16}^2 + x_1^2 + y_1^2 - x_6^2 - y_6^2 \end{pmatrix} \quad (1)$$

In here,

$\Delta T_{12} = T_2 - T_1$, $\Delta T_{13} = T_3 - T_1$, $\Delta T_{14} = T_4 - T_1$, $\Delta T_{15} = T_5 - T_1$, $\Delta T_{16} = T_6 - T_1$

4.2 Observation of infrasound due to volcanic eruptions

As a large-scale infrasound observation experiment, we measured the infrasound excited by volcanic eruptions in Sakurajima, Japan. Sakurajima is an active volcano located in the southern part of Kyushu Island, Japan, and it is the best infrasound observation environment in Japan because it erupts frequently.

As shown in Figure 7, four devices are set at each of the four observation points (A to D) around the Sakurajima area. The Japan Meteorological Agency announced that an explosive eruption was observed at 18:27 on January 9, 2019, in Sakurajima. Figure 8 shows the observation results of the four devices near the time when the eruption was reported. The figure was obtained by subtracting the DC component for easy comparison.

The most significant peaks were observed with an amplitude in the range of approximately 30–40 Pa in all the devices. This peak signal could be judged as infrasound generated by the volcanic eruptions. For each data, after passing a finite impulse response low-pass filter of order 256 and a cutoff frequency of 20 Hz, only the frequency range below 20 Hz (the bandwidth of infrasound) was extracted. Thereafter, the arrival time difference between each device was estimated using the phase-limited correlation method, and the sound source position was estimated. As in the experiment on estimating the sound source position in the fireworks case, the sound source position (u, v) was calculated using Equation (1). As a result, the coordinate (u, v) was found to be (5412, -1012), located approximately 93 m away from the actual sound position.

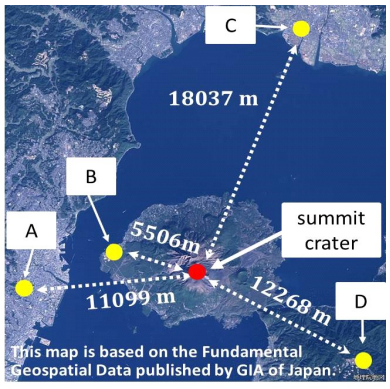

Figure 7 –Position of four observation points

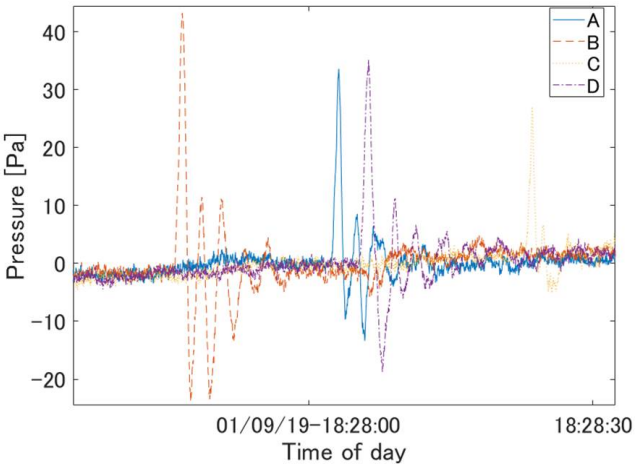

Figure 8 – Observation results for four devices

In this experiment, all devices could detect the infrasound, unlike that in the fireworks experiment, in which the peak signal amplitude was low, and the separation of noise and infrasound was an issue. The error in the infrasound source localization was found to be 93 m. Nevertheless, considering that volcanic eruptions have a scale of several thousand meters, the estimation of the sound source position is acceptably accurate. This suggests that estimating the sound source position in a real environment is possible for an infrasound with an amplitude of over 5 Pa (waveform noise).

5. CONCLUSIONS

In this study, we developed a new infrasound observation device stacked with eight low-cost MEMS atmospheric pressure sensors to improve the signal-to-noise ratio. We conducted multipoint observation experiments with indoor and outdoor field tests. In the indoor experiments, the accuracy of time synchronization was examined by positioning the infrasound observation devices at different points in a room. The results showed that the errors are within tolerable values.

In the outdoor field test, the infrasound excited by the explosion of fireworks during a festival was observed at multiple points in Sendai, Japan. The results showed that the source positions can be estimated with reasonable accuracy; however, a three-dimensional sound source estimation would be necessary to obtain better estimates. Furthermore, as a large-scale infrasound observation experiment, we measured the infrasound excited by the volcanic eruptions in Sakurajima, Japan. The results demonstrated that the source position can be estimated with reasonable accuracy for an infrasound with an amplitude of over 5 Pa (waveform noise). These results suggest the usability of the device in estimating the source position of *tsunami*-scale earthquakes.

ACKNOWLEDGMENTS

A part of this study was supported by the Ministry of Internal Affairs and Communications SCOPE (17150200).

REFERENCES

1. David G. Harkrider. Theoretical and observed acoustic-gravity waves from explosive sources in the atmosphere. Journal of Geophysical Research. 1964; 69(24): 742-748.
2. Takeshi Mikumo. Atmospheric pressure waves and tectonic deformation associated with the Alaskan earthquake of March 28. Journal of Geophysical Research. 1964; 73(6): 2009-2025.
3. Takeshi Mikumo, Takuo Shibutani, Alexis Le Pichon, Milton Garces, David Fee, Takahiro Tsuyuki, Shingo Watada, Wataru Morii. Low-frequency acoustic-gravity waves from coseismic vertical deformation associated with the 2004 Sumatra-Andaman earthquake (Mw = 9.2). 2008; 113: B12402.
4. Takashi Izumiya, Hiroyashi Nagaoka. Generation of gravity acoustic wave by a tunami and the possibility of tunami forecast. Proceedings of Coastal Engineering. 1994; 41: 241-245.
5. Shingo Watada, Takashi Kunugi, Kenji Hirata, Hiroko Sugioka, Kiwamu Nishida, Shoji Sekiguchi, Jun

Oikawa, Yoshinobu Tsuji, Hiroo Kanamori. Atmospheric pressure change associated with the 2003 Tokachi-Oki earthquake. Geophysical Research Letters. 2006; 33: L24306.
6. Shingo Watada, Hiroo Kanamori. Acoustic resonant oscillations between the atmosphere and the solid earth during the 1991 Mt. Pinatubo eruption. 2010; 115: B12319.
7. Makoto Tahira. Observation and propagation of infrasound. Acoustical Society of Japan. 2007; 428-433.
8. Takahiko Murayama, Masaki Kanao, Masa-Yuki Yamamoto, Yoshiaki Ishihara. Infrasound Signals and Their Source Location Inferred from Array Deployment in the Lützow-Holm Bay Region, East Antarctica. 2017; 8(2): 181-188.
9. Yuji Saito, Ryuichi Nishimura, Shuichi Sakamoto, Yôiti Suzuki. Performance evaluation of an infrasound observation device using MEMS atomospheric pressure sensor. RISP International Workshop on Nonlinear Circuits, Communications and Signal Processing (NCSP'18). 2018; 6PM1-3-4: 411-414.
10 A. Mahajan, M. Walworth. 3D position sensing using the differences in the time-of-flights from a wave source to various receivers. IEEE Transactions on Robotics and Automation. 2001; 17(1): 91-94.